Chloride-Mediated Apoptosis-Inducing Activity of Bis(sulfonamide) Anionophores

Tanmoy Saha,[†] Munshi Sahid Hossain,[†,§] Debasis Saha,[†] Mayurika Lahiri,[‡] and Pinaki Talukdar[*,†]

[†]Department of Chemistry, Indian Institute of Science Education and Research Pune, Pune, Maharashtra 411008, India
[‡]Department of Biology, Indian Institute of Science Education and Research Pune, Pune, Maharashtra 411008, India

Ⓢ *Supporting Information*

ABSTRACT: Transmembrane anion transport modality is enjoying a renewed interest because of recent advances toward anticancer therapy. Here we show bis(sulfonamides) as efficient receptors for selective Cl^- ion binding and transport across lipid bilayer membranes. Anion-binding studies by ^{1}H NMR indicate a logical correlation between the acidity of sulfonamide N−H proton and binding strength. Such recognition is influenced further by the lipophilicity of a receptor during the ion-transport process. The anion-binding and transport activity of a bis(sulfonamide) system are far superior compared to those of the corresponding bis-(carboxylic amide) derivative. Fluorescent-based assays confirm the Cl^-/anion antiport as the operational mechanism of the ion transport by bis(sulfonamides). Disruption of ionic homeostasis by the transported Cl^- ion, via bis(sulfonamide), is found to impose cell death. Induction of a caspase-dependent intrinsic pathway of apoptosis is confirmed by monitoring the changes in mitochondrial membrane potential, cytochrome *c* leakage, activation of family of caspases, and nuclear fragmentation studies.
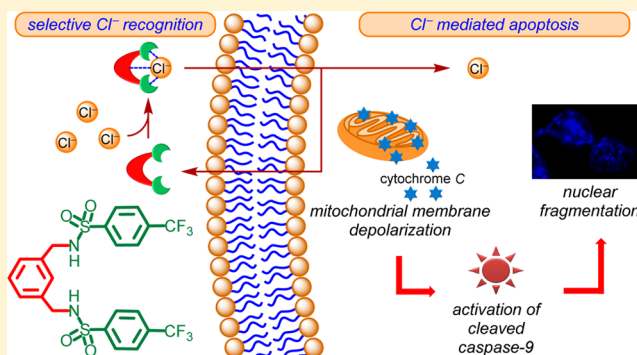
1. INTRODUCTION

Ion transport across a cell membrane controls the distribution of collective information stored in the building constituents of cells and performs specific functions.[1−5] Certain classes of membrane proteins, such as channels, carriers, etc., facilitate the ion transport process, overcoming the hydrophobic barrier of the phospholipid bilayer membranes.[6−8] Regulation of ion movement across the bilayer membranes is essential for neuronal proliferation, cellular signaling, pH control of osmotic pressure, etc.[9−11] Chloride, bicarbonate, and phosphate are the most abundant anions in physiological systems, and the typical extracellular (110 mM) versus intracellular (5−15 mM) concentration gradient of Cl^- ions is maintained by the transmembrane proteins.[12] Selective transport of Cl^- ions is indispensable for diverse biological processes, e.g., trans-epithelial salt transport, acidification of internal and extracellular compartments, cell volume regulation, cell cycle, and apoptosis.[13,14] On the other hand, misregulated transport of Cl^- ions, occasionally resulting from mutation of transmembrane proteins such as in the CFTR-Cl channel, etc., can cause life-shorting diseases like cystic fibrosis.[15] Furthermore, defects in anion transport proteins can lead to various diseases, e.g. Bartter syndrome, Gitelman syndrome, Dent's diseases, renal tubular acidosis, deafness, etc.[7,16]

Recently, the introduction of artificial ion channels as "channel replacement therapy" has been investigated as a novel combination treatment modality for targeting diseases associated with ion channel dysfunction.[17,18] Therefore, synthetic ion transport systems have immense potential in integrating a palliative care approach into several life-threatening diseases, including cystic fibrosis, cancer, etc. Prodigiosin[19] is a natural Cl^- carrier that can function as an anion exchanger via either H^+/Cl^- symport or Cl^-/anion antiport mechanism.[20] Ion transport properties of prodigiosin and its synthetic analogues are also linked to their anticancer activities.[21,22] Among diverse synthetic anionophores,[23−47] classes of urea/thiourea,[30,32,36] calix[4]pyrrole[27] derivatives, and tambjamine analogues[24] were also reported for their anticancer activities. These molecules either change the intracellular pH or disrupt the cellular ionic homeostasis, which triggers the apoptosis-inducing pathway. Here we demonstrate bis(sulfonamides) as a new class of low-molecular-weight Cl^- transporters. The study provides thoughtful insight into the correlation between structure, lipophilicity, anion recognition, and anion transport activity. Transport of Cl^- into the cells by these anionophores facilitates the activation of caspase-dependent apoptotic pathways.
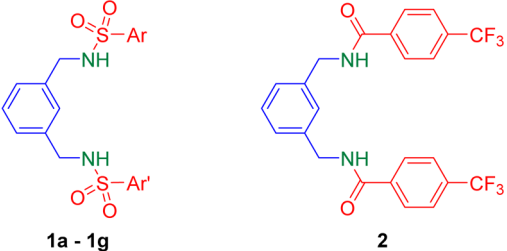
Sulfonamide was envisaged as a better scaffold for anion recognition compared to the carboxylic amide,[48,49] due to the higher acidity of the N−H proton.[50,51] The *m*-xylenediamine was selected as the rigid core, and the arylsulfonyl moieties

were varied to tune the N−H proton acidity as well as lipophilicity of bis(sulfonamide) derivatives. According to Lipinski's rule,[52] the structural modulation, based on lipophilicity, was expected to influence the membrane permeability of designed molecules; thereby, a variation in the ion transport activity was envisaged.[36,58] The logP values of all designed molecules were calculated (i.e., logP = 2.77, 2.96, 4.11, 3.69, 3.62, 4.84, and 5.06 for **1a−1g**, respectively) using the calculator plugins of MarvinSketch program (Table 1).[53] The

Table 1. Structures, logP Values, and pKₐ₁ Values of N−H Protons of Designed Anionophores 1a−1g and 2

Compound	ξ—Ar	ξ—Ar'	logP[a]	pKₐ₁[a]
1a	OMe	OMe	2.77	10.17
1b	NO₂	NO₂	2.96	9.97
1c	Me	Me	4.11	10.36
1d	Br	OMe	3.69	10.15
1e	Br	Br	3.62	10.13
1f	CF₃	CF₃	4.84	10.10
1g	naphthyl	naphthyl	5.06	10.23
2	-	-	5.33	13.23

[a]Calculator plugins of MarvinSketch program were used for structure−property prediction and calculation.

program was also used for predicting the pKₐ₁ value of sulfonamide N−H protons (Table 1). Bis(carboxylic amide) derivative **2** was designed to evaluate the importance of the sulfonamide groups in the anion recognition process.

2. RESULTS AND DISCUSSION

2.1. Synthesis. Compounds **1a−1g** were synthesized from commercially available *m*-xylenediamine **3** by treating with corresponding sulfonyl chloride derivatives (Scheme 1). Compound **2**, on the other hand, was synthesized from 4-(trifluoromethyl)benzoic acid **4** by treating with SOCl₂ followed by addition of **3**. All compounds were purified by column chromatography and characterized by ¹H NMR, ¹³C NMR, HRMS, IR, and melting point (see Supporting Information for detailed experiments and characterization).

2.2. Anion-Binding Studies. At first, Cl⁻ ion-binding properties of **1a−1g** and **2** were investigated by ¹H NMR

Scheme 1. Syntheses of (A) Bis(sulfonamide) Derivatives 1a−1g and (B) Bis(carboxylic amide) Derivative 2
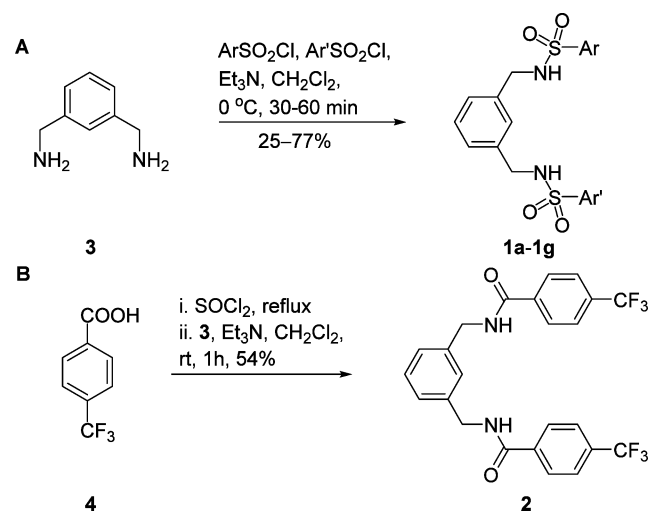
titrations in either CD₃CN (for **1a**, **1b**, **1c**, **1f**, **1g**, and **2**) or CDCl₃ (for **1d** and **1e**), selected based on compatibility. Upon stepwise addition of tetrabutylammonium chloride (TBACl) to compounds **1a−1g**, downfield shifts of Hₐ, H_b, and H_c signals and upfield shifts of H_d protons were observed (Figure 1 and
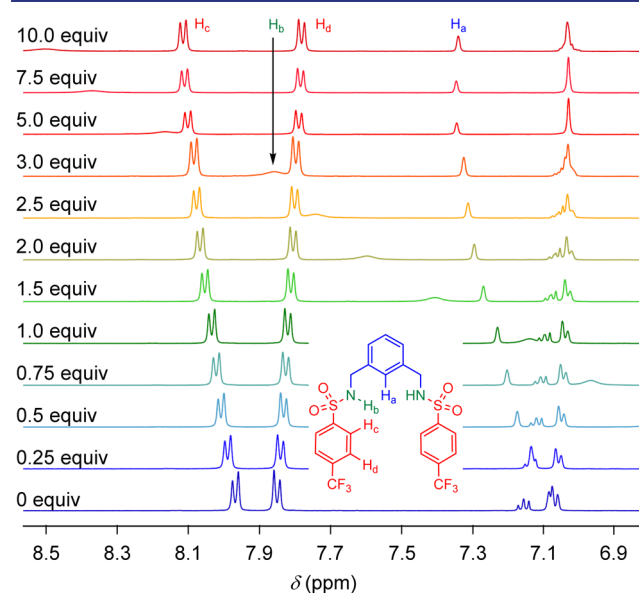

Figure 1. Partial ¹H NMR (400 MHz, 298 K) spectral change of **1f** in CD₃CN upon stepwise addition of TBACl (0−10 equiv).

Supporting Information, Figures S1−S7). These data indicate the presence of C−Hₐ···Cl⁻, N−H_b···Cl⁻, and C−H_c···Cl⁻ interactions with the anion. For calculating stoichiometry and binding constant, the change in chemical shift (Δδ) of Hₐ proton was monitored rather than the Δδ of H_b proton due to the line broadening of the H_b proton upon addition of excess TBACl. When the receptor **1f** and TBACl were mixed in CD₃CN by varying mole fraction (*x*) of the receptor (Table S1), and the Δδ of Hₐ proton was monitored (Figure S9A), the maximum interaction was observed at *x* = 0.5, indicating 1:1 complexation between **1f** and Cl⁻ (Figure S9B). The δ of the Hₐ proton from Figures S1−S7 was plotted against the increasing concentration of TBACl, and the association

constant for the complexation of **1f** with Cl⁻ was calculated by fitting the dose−response curve to the 1:1 binding model of WinEQNMR2 program.[54] The Cl⁻ ion recognition studies for **1a**, **1b**, **1c**, **1f**, and **1g** provided the dissociation constants, K_d = 21.28 ± 3.42, 2.56 ± 0.34, 19.50 ± 2.24, 2.39 ± 0.21, and 14.15 ± 0.81 mM, respectively. Similarly, Cl⁻ ion-binding studies with **1d** and **1e** in CDCl₃ provided K_d = 4.08 ± 0.44 and 2.48 ± 0.20 mM, respectively. Therefore, an electron withdrawing group on Ar/Ar′ moieties increases the acidity of sulfonamide N−H proton, and this is responsible for better Cl⁻ ion-binding. Halide ion-binding studies with **1f** provided the sequence Cl⁻ (K_d = 2.39 ± 0.21 mM) > Br⁻ (K_d = 19.47 ± 0.94 mM) > I⁻ ∼ F⁻ (K_d not determined), confirming better Cl⁻ ion recognition by the anionophore (Figure S10). It is noteworthy that the ¹H NMR titration of compound **2** with TBACl did not provide any significant change of proton chemical shift (Figure S8), suggesting poor Cl⁻ ion-binding by the bis(carboxylic amide) derivative. This observation was corroborated to the higher acidities of sulfonamide N−H protons (pK_{a1} = 10.10) of **1f** compared to the carboxylic amide N−H protons (pK_{a1} = 13.23) of **2**.

2.3. Anion-Binding Model.

To obtain the theoretical insight about the geometry of [**1f**+Cl⁻] complex, initial structures were generated by using CONFLEX 7 program.[55,56] Initial conformations for density functional theory (DFT) calculations were predicted by using MMFF94s force field of the software. First seven conformations, obtained according to their decreasing Boltzmann population percentages (Figure S11), were selected for further geometry optimization studies (see Supporting Information for details). The geometry optimization by Gaussian 09 program[57] using B3LYP functional and 6-311G++(d,p) basis set[58] provided the most stable conformation of the [**1f**+Cl⁻] complex (Figure 2A). This
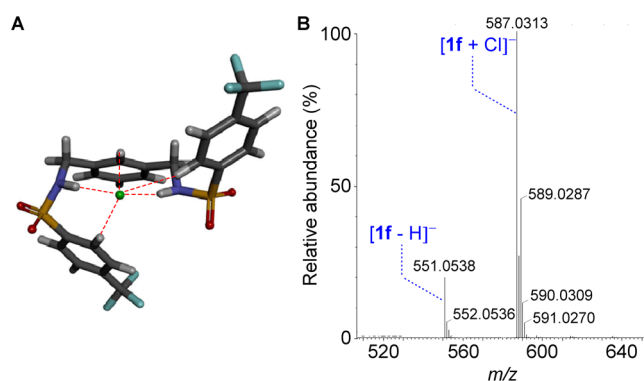

Figure 2. (A) Geometry-optimized structure of [**1f** + Cl⁻]. (B) Expanded region of the ESI-MS spectrum obtained by injecting the solution containing 1:1 mixture of **1f** and TBACl in CH₃CN.

optimized structure also correlates to the noncovalent interactions (i.e., two N−H···Cl⁻ and three C−H···Cl⁻ interactions) those observed in NMR titration studies. On the other hand, the direct experimental evidence of anion recognition of **1f** was obtained from the electrospray ionization-mass spectrometric (ESI-MS) study. A sample was prepared in CH₃CN by mixing **1f** and TBACl in 1:1 molar ratio, and electrosprayed under as mild as possible ionization conditions. The mass spectrometric data provided peaks at m/z = 587.0313 and 589.0287, which correspond to the [**1f**+Cl⁻] complex in the solution state (Figures 2B and S13).

2.4. Ion Transport Activity of 1a−1g and 2.

Anion recognition properties of bis(sulfonamide) compounds **1a−1g** encouraged us to evaluate their ion transport activity across large unilamellar vesicles (LUVs). The vesicles were prepared from egg-yolk phosphatidylcholine (EYPC) lipid with entrapped 8-hydroxypyrene-1,3,6-trisulfonate (HPTS, pK_a = 7.2) dye to get EYPC-LUVs⊃HPTS (Figure S14A).[59−61] Subsequently, a pH gradient, ΔpH = 0.6 (pH_{in} = 7.0 and pH_{out} = 7.6) was applied across the EYPC bilayer by adding NaOH in the extravesicular solution. The destruction of pH gradient by either H⁺ efflux or OH⁻ influx, upon addition of each compound, was monitored by measuring the fluorescence intensity of HPTS at λ_{em} = 510 nm (λ_{ex} = 450 nm). Finally, vesicles were collapsed by the addition of Titron X−100 to get the maximum fluorescence intensity (Figure S14B). All synthetic receptors **1a−1g** exhibited significant fluorescence intensity enhancement indicating transport of ions across the LUVs. Comparison of ion transport activity at identical concentration c = 10 μM provided the activity sequence: **1f** > **1e** > **1g** > **1d** > **1c** > **1b** > **1a** (Figure 3A). The dose−response
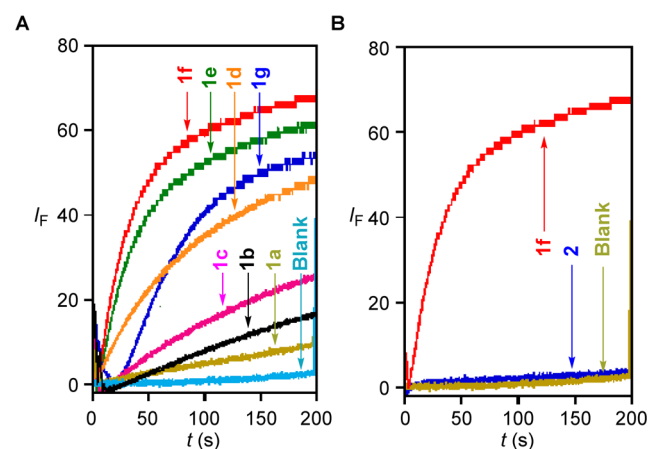

Figure 3. Comparison of ion transport activities of (A) bis-(sulfonamide) derivatives **1a−1g** (10 μM each) and (B) **1f** (10 μM) and **2** (10 μM) across EYPC-LUVs⊃HPTS.

plots of bis(sulfonamides) **1a−1f** (Figures S15−S20) provided EC₅₀ = 26.56 ± 1.13, 17.18 ± 0.77, 15.84 ± 0.23, 10.26 ± 0.42, 8.19 ± 0.11, and 5.89 ± 0.15 μM, respectively (Table 2). EC₅₀ calculation could not be performed on **1g** due to the precipitation observed at higher concentrations of the compound upon its addition in the buffer. The lowest activity of **1a** was primarily correlated to its poor anion-binding ability

Table 2. Experimentally Determined K_d and EC₅₀ Values for 1a−1g and 2

compound	logP	K_d (mM)	EC₅₀ (μM)
1a	2.77	21.28 ± 3.42[a]	26.56 ± 1.13
1b	2.96	2.56 ± 0.34[a]	17.18 ± 0.77
1c	4.11	19.50 ± 2.24[a]	15.84 ± 0.23
1d	3.69	4.08 ± 0.44[b]	10.26 ± 0.42
1e	3.62	2.48 ± 0.20[b]	8.19 ± 0.11
1f	4.84	2.39 ± 0.21[a]	5.89 ± 0.15
1g	5.06	14.15 ± 0.81[a]	ND[c]
2	5.33	ND[a,c]	ND[c]

[a]K_d values were determined in CD₃CN. [b]K_d values were determined in CDCl₃. [c]ND = could not be determined.

(K_d = 21.28 ± 3.42 mM). In addition to this, low logP = 2.77 of **1a** also contribute to its preferential distribution in the aqueous media over permeation through the hydrophobic lipid bilayer membranes. Compound **1c** with better Cl⁻-binding ability (K_d = 19.50 ± 2.24 mM) and permeability (logP = 4.11) compared to **1a** displayed higher transport activity. Although, the binding of **1b** with Cl⁻ is much higher than **1c**, the lower logP value of the nitro-substituted derivative restricts its membrane permeation which results in the poor ion transport property. Similarly, higher ion transport activity of the compound **1e** was corroborated to its better anion-binding ability than **1d**, even though they have close logP values. The effects of permeability (logP = 4.84) and anion-binding (K_d = 2.39 ± 0.21 mM) were most significant for **1f**, which provided the lowest value of EC_{50} = 5.89 μM. Despite having low anion-binding property (K_d = 14.15 ± 0.81 mM), appreciably high ion transport activity was observed for compound **1g**. This result can be justified from the highest logP value (logP = 5.06) among all bis(sulfonamide) compounds. However, the solubility of the compound **1g** in the aqueous solution was compromised because of its hydrophobic nature. On the other hand, ion transport activity of the bis(carboxylic amide) **2** was negligible compared to **1f** (Figure 3B). In spite of identical aromatic moieties and comparable logP values (logP = 4.84 and 5.33 for **1f** and **2**, respectively), higher acidity of sulfonamide N−H proton was crucial for better anion-binding by **1f**.

2.5. Ion Selectivity Studies. The top three active compounds **1d**−**1f** were used further to investigate the selectivity and the mechanism of ion transport. Ion transport activity across EYPC-LUVs⊃HPTS with intravesicular NaCl and iso-osmolar extravesicular NaA (where A⁻ = F⁻, Cl⁻, Br⁻, I⁻, NO₃⁻, SCN⁻, OAc⁻, and ClO₄⁻) was monitored to determine anion selectivity (Figure S22). Similarly, an iso-osmolar extravesicular MCl (where, M⁺ = Li⁺, Na⁺, K⁺, Rb⁺, and Cs⁺) was used to determine the selectivity among cations. The difference in ion transport activity upon changing extravesicular anions implies the involvement of anions in the transport process. For compound **1f** (c = 6 μM), an activity sequence: Cl⁻ ≫ SCN⁻ > OAc⁻ > F⁻ > ClO₄⁻ ≥ I⁻ > NO₃⁻ > Br⁻ was observed (Figures 4A and S23C). The observed Cl⁻
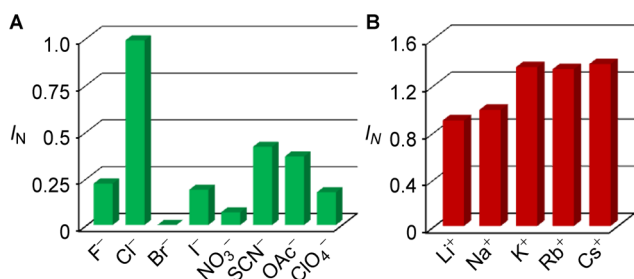

Figure 4. (A) Anion and (B) cation selectivity of **1f** (6 μM) determined from the ion transport studies across EYPC-LUVs⊃HPTS. The fluorescence intensity values at 100 s after addition of **1f** were normalized with respect to the intensity value obtained with extravesicular NaCl.

ion selectivity of **1f** rationalized by the strong binding of the ion in the cavity of the bis(sulfonamide) molecule. Lower transport activities for other anions indicate poor binding of these anions due to the mismatch of their sizes with the binding pocket of the bis(sulfonamide). The little-enhanced activity observed for I⁻ compared to Br⁻ may be because of the higher membrane

permeation of more hydrophobic I⁻ anion.[62] Variation of monovalent cations in the extravesicular buffer provided marginally enhanced ion transport activities for K⁺, Rb⁺, and Cs⁺ compared to Li⁺ and Na⁺ (Figures 4B and S24C). In the absence of any of ditopic binding motif in **1f**, the observations suggest the possibility of cation recognition as an alternate binding motif in the molecular cavity.[63] Anion selectivity studies for **1d** and **1e** also implied excellent transport of Cl⁻ ion (Figure S23A,B).

2.6. Chloride Leakage Studies. In the next stage, Cl⁻ ion transport activities of **1d**−**1f** across LUVs were investigated in details by monitoring the fluorescence intensity of intravesicular lucigenin dye at λ_{em} = 535 nm (λ_{ex} = 450 nm).[64] EYPC/cholesterol-LUVs⊃lucigenin were prepared with 7:3 EYPC/cholesterol by entrapping lucigenin dye and NaNO₃ (200 mM). Subsequently, a Cl⁻/NO₃⁻ gradient was applied by addition of concentrated solution of NaCl in the extravesicular buffer (Figure S25A). Quenching of lucigenin fluorescence due to the influx of Cl⁻ ion by bis(sulfonamides) was monitored with time. Finally, Triton X-100 was added to get the complete quenching of lucigenin fluorescence (Figure S25B). A sharp quenching in fluorescence, observed upon addition of **1f**, confirmed the Cl⁻ transport activity of the compound (Figure 5A). Compounds **1e** and **1d** also displayed quenching of
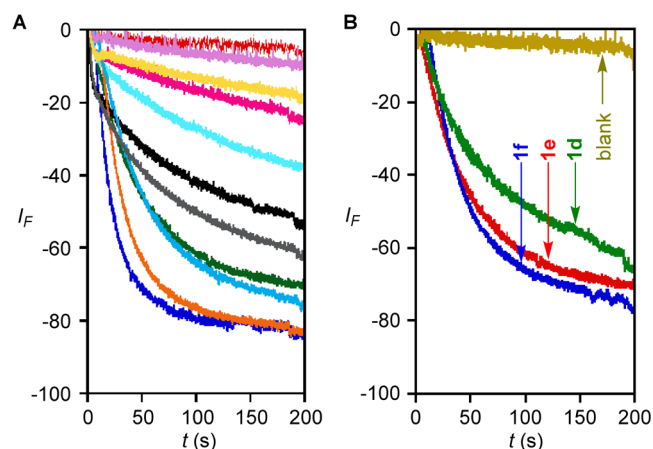

Figure 5. (A) Cl⁻ ion influx across EYPC/cholesterol-LUVs⊃lucigenin upon addition of **1f** (0−80 μM). (B) Comparison of Cl⁻ influx across EYPC/cholesterol-LUVs⊃lucigenin for **1d**, **1e**, and **1f** (60 μM each).

lucigenin fluorescence in the presence of extravesicular NaCl (Figure S26A,B), and the observed trend of Cl⁻ transport activity **1f** > **1e** > **1d** (Figure 5B) resembles that obtained from HPTS assays (Figure 3A).

Numerical analysis of the activity profiles (Figure 5B) were done to get the quantitative data of Cl⁻ ion transport across EYPC/cholesterol-LUVs⊃lucigenin. At first, the normalized fluorescence quenching curves were fitted to the single-exponential decay function (Equation S5), and then the half-life ($t_{1/2}$) was calculated by using eq S6 (Supporting Information). Similarly, the initial rate (r_i) was estimated by fitting the dose−response curve to a double exponential decay function (Equations S7 and S9). An increase in initial rate (r_i) with a concomitant decrease in half-life ($t_{1/2}$) was encountered while moving from compound **1d** to **1e** to **1f** (Table 3).

2.7. Ion Transport Mechanism. In the aforestated lucigenin experiments, either Cl⁻/NO₃⁻ antiport or Cl⁻/Na⁺

Table 3. Determination of Half-Life ($t_{1/2}$) and Initial Rate (r_i) Values of Cl⁻ Ion Influx across EYPC/Cholesterol-LUVs⊃Lucigenin by 1d–1f (60 μM Each)

compound	$t_{1/2}$ (s)	r_i (s⁻¹)
1d	32.36 ± 0.10	0.0165 ± 0.0014
1e	26.04 ± 0.09	0.0232 ± 0.0026
1f	17.86 ± 0.05	0.0335 ± 0.0087

symport was considered as the probable mechanism as the ion transport pathway. Therefore, experiments were carried out by varying either the cations or the anions in the extravesicular media to identify the correct mechanism. To evaluate the presence of a symport process, vesicles containing lucigenin in NaNO₃ were suspended in extravesicular MCl (M⁺ = Li⁺, Na⁺, K⁺, Rb⁺, and Cs⁺) salt solution (Figure S27). The addition of **1f** displayed small differences in the transport rates which rule out the possibility of Cl⁻/Na⁺ symport mechanism (Figure 6A). On
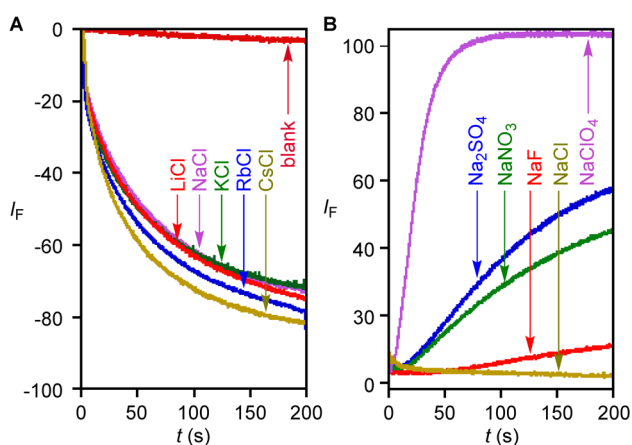

Figure 6. (A) Influx of Cl⁻ ion across EYPC/cholesterol-LUVs⊃lucigenin upon addition of **1f** (60 μM) with intravesicular NaNO₃ and extravesicular MCl (M⁺ = Li⁺, Na⁺, K⁺, Rb⁺, and Cs⁺). (B) Exflux of Cl⁻ ion across EYPC/cholesterol-LUVs⊃lucigenin upon addition of **1f** (40 μM) with intravesicular NaCl and extravesicular Na$_m$A salt (A⁻ = F⁻, Cl⁻, NO₃⁻, SO₄²⁻, and ClO₄⁻; m = valency of an anion).

the other hand, the variation of extravesicular of Na$_m$A (A⁻ = F⁻, ClO₄⁻, NO₃⁻, SO₄²⁻, Cl⁻; m = valency of an anion) with iso-osmolar intravesicular NaCl (Figure S28) provided remarkable differences in Cl⁻ efflux rates upon addition of **1f** (Figure 6B). These experiments suggest that the Cl⁻/A⁻ antiport is the effective ion transport process.

Finally, in pursuit of direct experimental insight of preferential transporting mechanism for **1f**, valinomycin (V), a K⁺-selective transporter, was used. EYPC/cholesterol-LUVs⊃lucigenin with intravesicular NaNO₃ were suspended in the KCl solution (Figure S29), and ion transport rate of **1f** was monitored in the absence and in the presence of valinomycin. A significant enhancement in the rate of transport was observed in the presence of valinomycin (Figure 7A). Numerical analysis of the normalized fluorescence quenching curves provided r_i = 0.0120 ± 0.0004 s⁻¹ and $t_{1/2}$ = 47.04 ± 0.14 s for only **1f**, whereas the combination of **1f** and valinomycin gave r_i = 0.1333 ± 0.0007 s⁻¹ and $t_{1/2}$ = 5.83 ± 0.02 s, indicating more than 11-fold enhancement in the Cl⁻ transport rate. The remarkable improvement of transport rate in the presence of valinomycin clearly indicates the Cl⁻/NO₃⁻

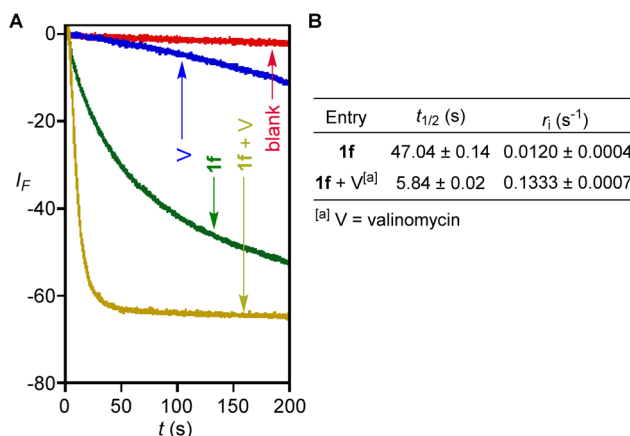| Entry	$t_{1/2}$ (s)	r_i (s⁻¹)
1f	47.04 ± 0.14	0.0120 ± 0.0004
1f + V[a]	5.84 ± 0.02	0.1333 ± 0.0007

[a] V = valinomycin

Figure 7. (A) Comparison of Cl⁻ transport activity of **1f** (40 μM) in the presence and in the absence of valinomycin (2.5 μM). (B) Calculated half-life ($t_{1/2}$) and initial rate (r_i) of Cl⁻ influx for **1f** in the presence and in the absence of valinomycin.

antiport mechanism of **1f**, which gets accelerated because of the synergistic effect of **1f** and valinomycin.

2.8. Evidence of Carrier Mechanism. The required evidence of ion transport through carrier mechanism was obtained through the classic U-tube experiment.[33,36,40,65] In this experiment the mimic of lipid membrane was established by an organic phase, separating two aqueous phases. The large dimension of organic phase restricts the movement of ions from one aqueous layer to the other whereas, ion carriers can easily act as a vehicle by overcoming the organic phase barrier. In each experiment, equimolar NaCl and NaNO₃ were added to the aqueous phase of the donor and receiver phase, respectively. Remarkable enhancement in Cl⁻ level was observed in the receiver aqueous phase only when **1f** was taken in the organic phase (Figures 8 and S30). This result confirm the Cl⁻ transport of **1f** by carrier mechanism.
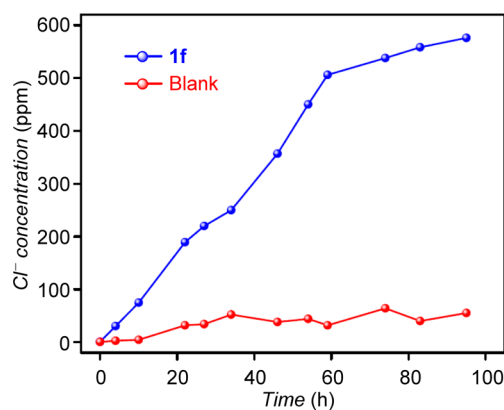

Figure 8. Concentration of Cl⁻ in the aqueous phase of receiver end of U-tube as the function of time. Data were recorded in the presence and in the absence of **1f** in the organic phase.

2.9. Effect of Ion Transport in Biological Systems. The excellent Cl⁻ transport activity of designed bis(sulfonamide) derivatives **1a**–**1f** prompted us to explore their bioapplicability. Recent studies have demonstrated that dysregulation of ionic homeostasis, via the influx of Cl⁻ ion into cells, can induce apoptosis.[27,66,67] At first, the viability of various cancer (e.g., human breast cancer MCF-7, human bone osteosarcoma

U2OS, human cervical cancer HeLa, and lung adenocarcinoma epithelial A549) and normal (e.g., mouse fibroblast NIH3T3) cell lines were screened for compounds **1a**−**1f** and **2**. A single-point screening was done by MTT assay with these compounds (20 μM each). The maximum cell death was observed for the most efficient anionophore **1f** while the least active bis-(carboxylic amide) derivative **2** caused minimum cell death (Figure 9). Overall, the differences in cell viability were
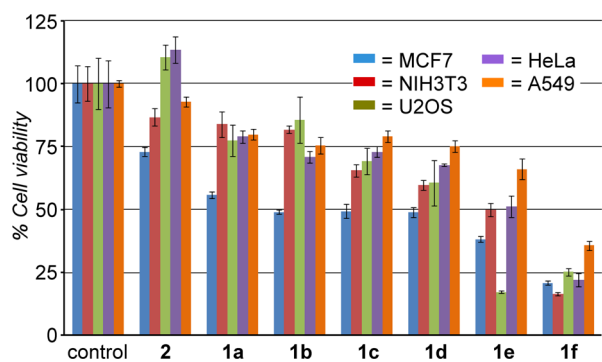

Figure 9. Cell viability obtained from single point screening of compounds **1a**−**1f** and **2** (20 μM each) by MTT assay. Cell viability was checked after 24 h treatment of each compound in various cell lines: from left to right, MCF7, NIH3T3, U2OS, HeLa, and A549. Each bar diagram represents mean cell viability, calculated from three independent experiments. Compound **1g** was excluded because of the precipitation in higher concentration.

inversely proportional to the ion transport abilities of these molecules. The dose-dependent cell viability studies for compounds **1e** and **1f** provided IC_{50} = 56.9−14.6 μM (Figure S31) and IC_{50} = 12.2−7.5 μM (Figure S32 and Table S3), respectively, depending on cell lines used. The compound **1f** was selected to perform the further studies because of its least IC_{50} values in the cell viability experiments.

The direct evidence of Cl^- ion transport into the live cells upon treatment with **1f** was obtained by using MQAE, a Cl^--selective dye (λ_{ex} = 350 nm and λ_{em} = 460 nm), that gives quenching of fluorescence in the presence of the ion.[68,69] A remarkable stepwise quenching of fluorescence was observed upon post incubation of either HeLa (Figure 10A) or MCF7 (Figure 10B) cells with **1f** (0−50 μM). The gradual quenching
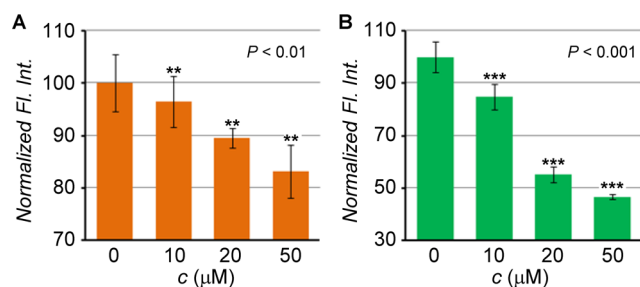

Figure 10. Normalized fluorescence intensity of (A) HeLa and (B) MCF7 cells incubated with MQAE (5 mM) for 3 h followed by treatment of **1f** (0−50 μM) for 24 h. Fluorescence intensities were recorded by the plate reader at λ_{em} = 460 nm (λ_{ex} = 350 nm) and normalized with respect to the fluorescence intensity of untreated cells. Each bar represents the mean intensity of three independent experiments, and the differences in mean intensity are statistically significant ($P < 0.01$ for HeLa and $P < 0.001$ for MCF7) according to one-way analysis of variance (ANOVA).

of MQAE fluorescence indicates a concentration-dependent influx of Cl^- ion in the intracellular matrix facilitated by the transporter molecule.

The correlation between the enhanced Cl^- ion level in the intracellular matrix, and the death of either HeLa or MCF7 cells was evaluated by altering the Cl^- ion concentration in the extracellular matrix. HBSS (Hank's balanced salt solution) buffers of two different salt compositions (with and without Cl^- ions) were prepared, and cells were suspended separately in these buffers. Then, both sets of cells were treated separately with **1f** (0−20 μM) for 24 h, and the cell viability between the sets was compared. Remarkably higher viability was observed for cells suspended in Cl^- ion free HBSS than those dispersed in the HBSS buffer containing the ion (Figure 11). These
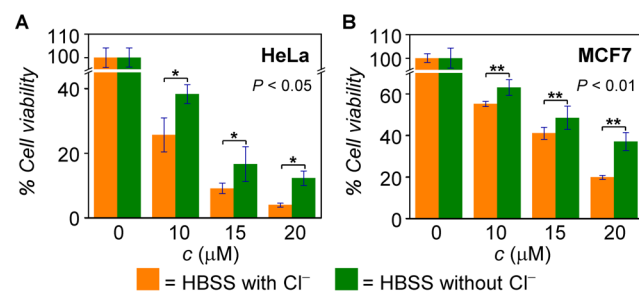

Figure 11. (A) Comparison of HeLa cell viability in Cl^--containing and Cl^--free HBSS buffer upon dose-dependent treatment of **1f** (0−20 μM) for 24 h. (B) Similar studies were done with MCF7 cells. Each bar represents the mean intensity of three independent experiments, and the differences in mean intensities are statistically significant ($P < 0.05$ for HeLa and $P < 0.01$ for MCF7) according to one-way analysis of variance (ANOVA).

results confirm that the enhanced level of intracellular Cl^- ion, transported by **1f**, is potentially related to the amount of cell death. Such Cl^- ion-mediated cell death is known to trigger the apoptotic pathways in live cells.[24,27,66,70]

A number of experiments have been carried out to demonstrate the appropriate apoptotic pathway. In the intrinsic pathway of apoptosis, disruption of mitochondrial membrane potential (MMP) induces the release of cytochrome c from mitochondria to cytosol.[71,72] Released cytochrome c subsequently binds to the Apaf-1 to form apoptosome. Then the cytochrome c/Apaf-1 complex activates caspase-9, which further activates multiple pathways, including activation of caspase-3, to induce apoptosis.[73−76] Therefore, the process of apoptosis can be monitored at several stages, e.g., (a) by monitoring the mitochondrial membrane potential (MMP) and cytochrome c release as a pre-apoptotic symptom, (b) by monitoring proteins of the caspase family involving in the caspase cascade mechanism, and (c) by observing the nuclear fragmentation of the cells. The collapse of MMP, observed during the early stages of apoptosis, can be monitored by using JC-1, a membrane potential sensitive fluorescent probe.[77,78] This dye exhibits intense red fluorescence when present in the mitochondrial membrane of healthy cells due to the formation of J-aggregate. The disruption of MMP does not allow the dye to stay in the membrane resulting in its dispersion in the cytosol. In the cytoplasm, the JC-1 dye exhibits green fluorescence due to the loss of aggregation. When HeLa cells were treated with **1f** (0−20 μM) for 24 h followed by staining with JC-1, a stepwise decrease in the red fluorescence with concomitant enhancement of the green fluorescence was

observed (Figure 12A−C). Subsequently, the ratio of pixel intensities (i.e., red/green) was calculated from the live cell
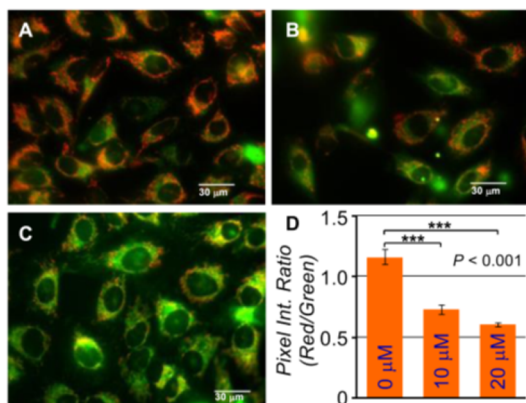

Figure 12. Live cell imaging of HeLa cells upon treating with (A) 0, (B)10, and (C) 20 μM **1f** for 24 h followed by staining with JC-1 dye. Each image was generated by merging the images obtained from red and green channels. (D) Bar graph representing the ratio of pixel intensities (red/green) for each set of cells. One-way ANOVA analysis of seven replicate images shows the statistically significant ($P < 0.001$) mean difference in the ratio of pixel intensity.

images of the stained cells (Figure 12D). The decrease in the ratio of pixel intensities can be correlated to the disruption of MMP upon treatment of **1f**.

Cytochrome *c* is a well-conserved electron-transport protein confined between mitochondrial intermembrane spaces. Apoptotic stimulation triggers the release of cytochrome *c* from mitochondria, which subsequently instigates the caspase-dependent apoptotic pathway.[79−81] HeLa cells were incubated with increasing concentration of **1f** (0, 10, and 20 μM) for 8 h, and immunostaining analysis was done with cytochrome *c* antibody. The release of cytochrome *c* was monitored by enhancement in emission intensity, which further diffused upon treatment with a higher dose. The release of cytochrome *c* upon ion transport endorses the induction of mitochondrial-dependent apoptosis by **1f** (Figure 13).
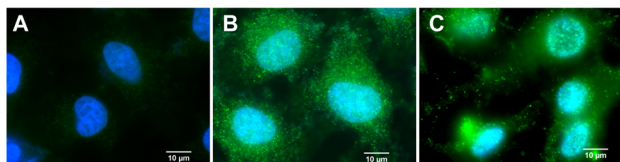

Figure 13. HeLa cells, treated first with (A) 0, (B) 10, and (C) 20 μM **1f** for 8 h, then fixed and analyzed for cytochrome *c* release by immunostaing with cytochrome *c* antibody. DMSO was used as negative control, and the nuclei were stained with Hoechst 33342.

It is already established that the mitochondria-dependent apoptotic pathway can proceed via activation of family of caspases.[75,82−84] In the next step, for better understanding of ion-transporter-induced caspase cascade, the activation of initiator caspase-9 and the executioner caspase-3 was investigated. Immunoblot assay was performed on HeLa cells upon treatment with **1f** (0−40 μM) for 24 h by using appropriate primary antibodies. A dose-dependent enhancement of the amount of activated caspase-9 and caspase-3 with simultaneous degradation of procaspase-3 indicates the caspase-dependent intrinsic pathway of the apoptosis program (Figures

14 and S33). On the other hand apoptosis can also be initiated via extrinsic pathway involving caspase-8.[75,85] No such
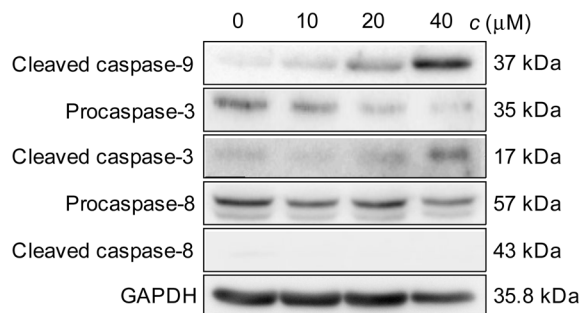

Figure 14. Immunoblot assay for active caspase-9, caspase-3, and caspase-8 in HeLa cells, after 24 h incubation with various concentrations (0, 10, 20, and 40 μM) of **1f**. Data were quantified with respect to glyceraldehyde 3-phosphate dehydrogenase (GAPDH) levels.

activation of caspase-8, and no degradation of procaspase-8, ruled out the possibility of extrinsic pathway of apoptosis program (Figures 14 and S33B). Similarly, apoptosis can also proceed via activation of p53-mediated pathway.[86] Posphorilation at Ser-15 position of the p53 protein is a common phenomenon in p53-mediated apoptosis pathway.[87] Absence of phosphorilation at Ser-15 position of p53 protein, monitored by immunoblot assay, eliminate the possibility of p53-mediated apoptosis program (Figure S34).

Moreover, to elucidate the caspase-dependent intrinsic pathway of apoptosis, cell viability was screened in the presence of caspase inhibitors. The small polypeptide derivatives benzyloxycarbonyl-Asp(OMe)-Glu(OMe)-Val-Asp(OMe)-fluoromethylketone (z-DEVD-fmk) and benzyloxycarbonyl-Leu-Glu(OMe)-His-Asp(OMe)-fluoromethylketone (z-LEHD-fmk) are known cell-permeable, irreversible inhibitors for caspase-3 and caspase-9, respectively, which can inhibit the caspase-dependent apoptotic pathway of cell.[83,88,89] Almost negligible amount of caspase-3 and caspase-9 activation was observed in immunoblot assay, upon pre-incubation of HeLa cells with z-DEVD-fmk and z-LEHD-fmk (50 μM each) followed by treatment of **1f** (20 μM) for 24 h (Figures 15A and S35). Similarly, in MTT assay, significant increase in cell viability was encountered upon treatment of **1f** when cells were pre-incubated with caspase inhibitors (Figure 15B). This enhanced cell viability can be correlated to the protection process of cells form ion transporters by inhibition of caspase-dependent intrinsic pathway of apoptosis program.

Apoptosis can also be characterized by distinct changes in cellular morphology, including membrane blebbing, chromatin condensation, the appearance of membrane-associated apoptotic bodies, and internucleosomal DNA fragmentation, as well as by cleavage of poly(ADP-ribose) polymerase (PARP).[36,90,91] Nuclear condensation, fragmentation, and formation of apoptotic bodies can be identified by Hoechst 33342, a fluorescent nuclear staining dye. HeLa cells were treated with **1f** (20 μM) for 24 h and then stained with the dye. A significant change in nuclear morphology was observed in treated HeLa cells compared to untreated ones (Figure 16). The appearance of nuclear condensation and fragmentation indicates apoptotic cell death.

It is also well-known that PARP cleavage, by endogenous caspases, serves to prevent futile repair of DNA strand breaks
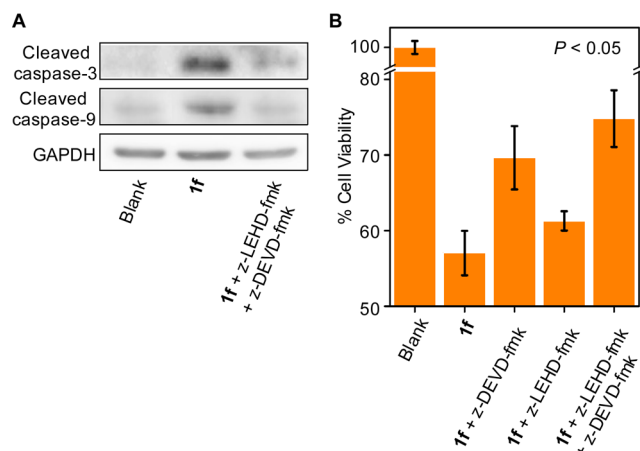
Figure 15. (A) Immunoblot analysis of HeLa cells pre-incubated with z-DEVD-fmk and/or z-LEHD-fmk (50 μM each) for 3 h followed by incubation with **1f** (20 μM) for 24 h. Difference in cell viability upon treatment with **1f** and caspase inhibitors measured by MTT assay. (B) HeLa cells were pre-incubated with z-DEVD-fmk and/or z-LEHD-fmk (50 μM each) for 3 h followed by incubation with **1f** (10 μM) for 24 h. Each bar represents the mean intensity of three independent experiments, and the differences in mean intensity are statistically significant ($P < 0.05$), in each case, according to one-way analysis of variance (ANOVA).
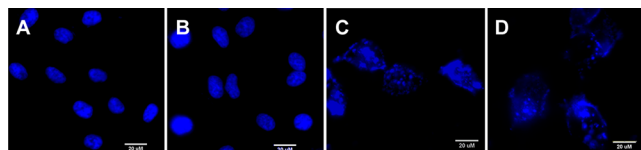

Figure 16. Live cell imaging of HeLa cells stained with Hoechst 33342. (A,B) Typical oval nuclei in control (untreated) cells and (C,D) fragmented nuclei of cells after 24 h treatment with **1f** (20 μM).

during the apoptotic program.[90,92] An appearance of cleaved PARP-1 (86 kDa) with concomitant degradation of full-length PARP-1 (116 kDa) was observed upon treatment of HeLa cells with **1f** (40 μM) for 24 h (Figure 17). The activation of cleaved PARP-1 by endogenous caspase substrate can be considered as an additional validation of caspase-mediated apoptosis.
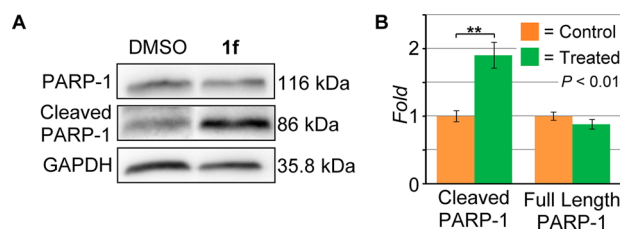

Figure 17. (A) Expression of cleaved PARP-1 and degradation of full length PARP-1 in HeLa cells, after 24 h incubation with **1f** (40 μM), determined by immunoblot analysis. (B) Statistically significant difference in cleaved PARP-1 expression was observed upon applying unpaid t-test on three replicate data.

Finally, to establish the relation between the change in ionic homeostasis and induction of apoptosis, reactive oxygen species (ROS) level of cells were measured. It is well known from the literature that the ROS level of a cell can be affected by changes in ionic homeostasis via interruption of the respiratory chain in mitochondria.[93,94] ROS levels in HeLa cells were measured

fluorometrically by using a ROS-sensitive probe, 3-methyl-7-(4,4,5,5-tetramethyl-1,3,2-dioxaborolan-2-yl)-2H-chromen-2-one (**ROS probe**).[95,96] An enhancement of ROS level was observed when HeLa cells were incubated with increasing concentrations of **1f** (0−100 μM) for 8 h (Figure 18A).
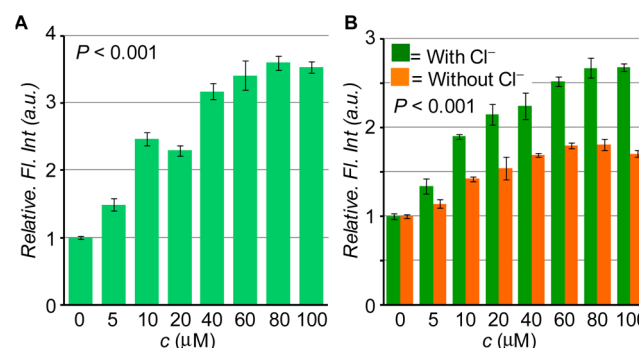

Figure 18. (A) Measurement of ROS production in HeLa cells upon incubation with varied concentrations of **1f** (0−100 μM) for 7 h, followed by treatment with the **ROS probe** (50 μM) for 1 h in the same solution. (B) Comparison of ROS production in HeLa cells in the absence and in the presence of Cl^- ion (HBSS buffer with and without Cl^- ion) in extracellular media. Fluorescence intensities were recorded from the plate reader at λ_{em} = 460 nm (λ_{ex} = 315 nm) and normalized with respect to the fluorescence intensity of untreated cells. Each bar represents the mean intensity of three independent experiments, and the differences in mean intensity are statistically significant ($P < 0.001$), in each case, according to one-way analysis of variance (ANOVA).

Furthermore, a significantly higher enhancement in ROS level was observed when medium with Cl^- was used as external buffer (HBSS buffer with Cl^-) than when Cl^--free medium was used (Cl^--free HBSS buffer) (Figure 18B). Thus, the Cl^--dependent enhancement of ROS level signifies the ion-transport-mediated ROS production in HeLa cells upon incubation with **1f**. The enhanced ROS level instigates the opening of the mitochondrial permeability transition pore, which results in the leakage of cytochrome c from mitochondria, i.e., the induction of intrinsic apoptotic pathway.[97−100]

3. CONCLUSION

In this study, we have described bis(sulfonamides) as efficient artificial anionophores for selective Cl^- ion transport. These anion transporters were synthesized by reacting the 1,3-phenylenedimethanamine core with arylsulfonyl chlorides to create a molecular library of varied sulfonamide N−H proton acidity and lipophilicity. ^{1}H NMR titrations confirmed strong anion binding when an electron-withdrawing group was connected to the arylsulfonyl group. The bis(sulfonamide) system displayed the strongest binding with Cl^- ion compared to other halides, and a 1:1 binding model was established with Cl^- ion. Anion recognition of the system was also much stronger compared to that of the corresponding bis(carboxylic amide) derivative. Transmembrane ion transport studies confirmed that the compound with appropriate lipophilicity and strong anion-binding ability is the most efficient transporter. Selective transport of Cl^- ion and Cl^-/anion antiport mechanism across large unilamellar vesicles were also confirmed by several fluorescence-based assays.

MTT assay indicated an inverse correlation between cell viability and ion transport activity of bis(sulfonamides) derivatives. The elevated intracellular Cl^- ion level and the Cl^--mediated cell death were also confirmed. The disruption of ionic homeostasis of cells led to the change in the mitrochondrial membrane potential, which subsequently initiated the release of cytochrome *c* from mitochondrial intermembrane spaces to cytosol. The mitochondria-dependent intrinsic apoptotic pathway of cell death was confirmed by expression of a family of caspases and cleaved PARP-1. The change in nuclear morphology was also observed as a post-apoptotic symptom. The caspase-9- and caspase-3-dependent intrinsic pathway of apoptosis was further confirmed by monitoring transporter-mediated cell death in the presence of caspase inhibitors. Finally, the induction of apoptosis mechanism by ion transport involving excessive production of ROS was demonstrated. Hence, artificial Cl^- transporters as apoptotic inducing agents, via disrupting ionic homeostasis of cell, could be a potential therapeutic tool for cancer treatment in the next generation.

■ ASSOCIATED CONTENT

Ⓢ Supporting Information

The Supporting Information is available free of charge on the ACS Publications website at DOI: 10.1021/jacs.6b01723.

Experimental procedures, compound characterization data, theoretical calculations, and biological evaluation and data (PDF)

■ AUTHOR INFORMATION

Corresponding Author

*ptalukdar@iiserpune.ac.in

Present Address

§M.S.H.: Department of Chemical Sciences, Indian Institute of Science Education and Research Kolkata, Mohanpur, West Bengal 741246, India

Notes

The authors declare no competing financial interest.

■ ACKNOWLEDGMENTS

■ REFERENCES

(1) Allen, T. W.; Andersen, O. S.; Roux, B. *Proc. Natl. Acad. Sci. U. S. A.* **2004**, *101*, 117.

(2) Agre, P. *Angew. Chem., Int. Ed.* **2004**, *43*, 4278.

(3) MacKinnon, R. *Angew. Chem., Int. Ed.* **2004**, *43*, 4265.

(4) Pinto, L. H.; Dieckmann, G. R.; Gandhi, C. S.; Papworth, C. G.; Braman, J.; Shaughnessy, M. A.; Lear, J. D.; Lamb, R. A.; DeGrado, W. F. *Proc. Natl. Acad. Sci. U. S. A.* **1997**, *94*, 11301.

(5) Smart, O. S.; Breed, J.; Smith, G. R.; Sansom, M. S. P. *Biophys. J.* **1997**, *72*, 1109.

(6) Diamond, J. M.; Wright, E. M. *Annu. Rev. Physiol.* **1969**, *31*, 581.

(7) Hladky, S. B.; Haydon, D. A. Ion Movement in Gramicidin Channels. In *Current Topics in Membranes and Transport*; Bronner, F., Ed.; Academic Press, New York, 1984; Vol. *21*, pp 327−372.

(8) Song, L.; Hobaugh, M. R.; Shustak, C.; Cheley, S.; Bayley, H.; Gouaux, J. E. *Science* **1996**, *274*, 1859.

(9) Chiu, S. Y.; Wilson, G. F. *J. Physiol.* **1989**, *408*, 199.

(10) DeCoursey, T. E.; Chandy, K. G.; Gupta, S.; Cahalan, M. D. *Nature* **1984**, *307*, 465.

(11) Lange, K. *J. Cell. Physiol.* **2000**, *185*, 21.

(12) Davis, A. P.; Sheppard, D. N.; Smith, B. D. *Chem. Soc. Rev.* **2007**, *36*, 348.

(13) Duran, C.; Thompson, C. H.; Xiao, Q.; Hartzell, H. C. *Annu. Rev. Physiol.* **2010**, *72*, 95.

(14) Benz, R.; Hancock, R. E. W. *J. Gen. Physiol.* **1987**, *89*, 275.

(15) Choi, J. Y.; Muallem, D.; Kiselyov, K.; Lee, M. G.; Thomas, P. J.; Muallem, S. *Nature* **2001**, *410*, 94.

(16) Vaughan-Jones, R. D.; Spitzer, K. W.; Swietach, P. *J. Mol. Cell. Cardiol.* **2009**, *46*, 318.

(17) Broughman, J. R.; Shank, L. P.; Takeguchi, W.; Schultz, B. D.; Iwamoto, T.; Mitchell, K. E.; Tomich, J. M. *Biochemistry* **2002**, *41*, 7350.

(18) Saeed, Z.; Wojewodka, G.; Marion, D.; Guilbault, C.; Radzioch, D. *Curr. Pharm. Des.* **2007**, *13*, 3252.

(19) Fuerstner, A. *Angew. Chem., Int. Ed.* **2003**, *42*, 3582.

(20) Seganish, J. L.; Davis, J. T. *Chem. Commun.* **2005**, 5781.

(21) Sessler, J. L.; Eller, L. R.; Cho, W.-S.; Nicolaou, S.; Aguilar, A.; Lee, J. T.; Lynch, V. M.; Magda, D. J. *Angew. Chem., Int. Ed.* **2005**, *44*, 5989.

(22) Marchal, E.; Rastogi, S.; Thompson, A.; Davis, J. T. *Org. Biomol. Chem.* **2014**, *12*, 7515.

(23) Lisbjerg, M.; Valkenier, H.; Jessen, B. M.; Al-Kerdi, H.; Davis, A. P.; Pittelkow, M. *J. Am. Chem. Soc.* **2015**, *137*, 4948.

(24) Soto-Cerrato, V.; Manuel-Manresa, P.; Hernando, E.; Calabuig-Fariñas, S.; Martínez-Romero, A.; Fernández-Dueñas, V.; Sahlholm, K.; Knöpfel, T.; García-Valverde, M.; Rodilla, A. M.; Jantus-Lewintre, E.; Farràs, R.; Ciruela, F.; Pérez-Tomás, R.; Quesada, R. *J. Am. Chem. Soc.* **2015**, *137*, 15892.

(25) Valkenier, H.; Judd, L. W.; Li, H.; Hussain, S.; Sheppard, D. N.; Davis, A. P. *J. Am. Chem. Soc.* **2014**, *136*, 12507.

(26) Valkenier, H.; Haynes, C. J. E.; Herniman, J.; Gale, P. A.; Davis, A. P. *Chem. Sci.* **2014**, *5*, 1128.

(27) Ko, S.-K.; Kim, S. K.; Share, A.; Lynch, V. M.; Park, J.; Namkung, W.; Van Rossom, W.; Busschaert, N.; Gale, P. A.; Sessler, J. L.; Shin, I. *Nat. Chem.* **2014**, *6*, 885.

(28) Cooper, J. A.; Street, S. T. G.; Davis, A. P. *Angew. Chem., Int. Ed.* **2014**, *53*, 5609.

(29) Busschaert, N.; Bradberry, S. J.; Wenzel, M.; Haynes, C. J. E.; Hiscock, J. R.; Kirby, I. L.; Karagiannidis, L. E.; Moore, S. J.; Wells, N. J.; Herniman, J.; Langley, G. J.; Horton, P. N.; Light, M. E.; Marques, I.; Costa, P. J.; Felix, V.; Frey, J. G.; Gale, P. A. *Chem. Sci.* **2013**, *4*, 3036.

(30) Moore, S. J.; Haynes, C. J. E.; Gonzalez, J.; Sutton, J. L.; Brooks, S. J.; Light, M. E.; Herniman, J.; Langley, G. J.; Soto-Cerrato, V.; Perez-Tomas, R.; Marques, I.; Costa, P. J.; Felix, V.; Gale, P. A. *Chem. Sci.* **2013**, *4*, 103.

(31) Shang, J.; Si, W.; Zhao, W.; Che, Y.; Hou, J.-L.; Jiang, H. *Org. Lett.* **2014**, *16*, 4008.

(32) Moore, S. J.; Wenzel, M.; Light, M. E.; Morley, R.; Bradberry, S. J.; Gomez-Iglesias, P.; Soto-Cerrato, V.; Perez-Tomas, R.; Gale, P. A. *Chem. Sci.* **2012**, *3*, 2501.

(33) Busschaert, N.; Kirby, I. L.; Young, S.; Coles, S. J.; Horton, P. N.; Light, M. E.; Gale, P. A. *Angew. Chem., Int. Ed.* **2012**, *51*, 4426.

(34) Lin, N.-T.; Vargas Jentzsch, A.; Guenee, L.; Neudorfl, J.-M.; Aziz, S.; Berkessel, A.; Orentas, E.; Sakai, N.; Matile, S. *Chem. Sci.* **2012**, *3*, 1121.

(35) Bahmanjah, S.; Zhang, N.; Davis, J. T. *Chem. Commun.* **2012**, *48*, 4432.

(36) Busschaert, N.; Wenzel, M.; Light, M. E.; Iglesias-Hernández, P.; Pérez-Tomás, R.; Gale, P. A. *J. Am. Chem. Soc.* **2011**, *133*, 14136.

(37) Andrews, N. J.; Haynes, C. J. E.; Light, M. E.; Moore, S. J.; Tong, C. C.; Davis, J. T.; Harrell, W. A., Jr; Gale, P. A. *Chem. Sci.* **2011**, *2*, 256.

(38) Vargas Jentzsch, A.; Emery, D.; Mareda, J.; Metrangolo, P.; Resnati, G.; Matile, S. *Angew. Chem., Int. Ed.* **2011**, *50*, 11675.

(39) Wenzel, M.; Light, M. E.; Davis, A. P.; Gale, P. A. *Chem. Commun.* **2011**, *47*, 7641.

(40) Gale, P. A.; Tong, C. C.; Haynes, C. J. E.; Adeosun, O.; Gross, D. E.; Karnas, E.; Sedenberg, E. M.; Quesada, R.; Sessler, J. L. *J. Am. Chem. Soc.* **2010**, *132*, 3240.

(41) Busschaert, N.; Gale, P. A.; Haynes, C. J. E.; Light, M. E.; Moore, S. J.; Tong, C. C.; Davis, J. T.; Harrell, W. A., Jr. *Chem. Commun.* **2010**, *46*, 6252.

(42) Winstanley, K. J.; Allen, S. J.; Smith, D. K. *Chem. Commun.* **2009**, 4299.

(43) Fisher, M. G.; Gale, P. A.; Hiscock, J. R.; Hursthouse, M. B.; Light, M. E.; Schmidtchen, F. P.; Tong, C. C. *Chem. Commun.* **2009**, 3017.

(44) McNally, B. A.; Koulov, A. V.; Lambert, T. N.; Smith, B. D.; Joos, J.-B.; Sisson, A. L.; Clare, J. P.; Sgarlata, V.; Judd, L. W.; Magro, G.; Davis, A. P. *Chem. - Eur. J.* **2008**, *14*, 9599.

(45) Tong, C. C.; Quesada, R.; Sessler, J. L.; Gale, P. A. *Chem. Commun.* **2008**, 6321.

(46) Santacroce, P. V.; Davis, J. T.; Light, M. E.; Gale, P. A.; Iglesias-Sánchez, J. C.; Prados, P.; Quesada, R. *J. Am. Chem. Soc.* **2007**, *129*, 1886.

(47) Lee, J. H.; Lee, J. H.; Choi, Y. R.; Kang, P.; Choi, M.-G.; Jeong, K.-S. *J. Org. Chem.* **2014**, *79*, 6403.

(48) Berryman, O. B.; Hof, F.; Hynes, M. J.; Johnson, D. W. *Chem. Commun.* **2006**, 506.

(49) Mammoliti, O.; Allasia, S.; Dixon, S.; Kilburn, J. D. *Tetrahedron* **2009**, *65*, 2184.

(50) Huang, X.-Y.; Wang, H.-J.; Shi, J. *J. Phys. Chem. A* **2010**, *114*, 1068.

(51) http://www.chem.wisc.edu/areas/reich/pkatable/index.htm

(52) Lipinski, C. A.; Lombardo, F.; Dominy, B. W.; Feeney, P. J. *Adv. Drug Delivery Rev.* **1997**, *23*, 3.

(53) *Marvin 5.8.0*, ChemAxon, 2012 (http://www.chemaxon.com).

(54) Hynes, M. J. *J. Chem. Soc., Dalton Trans.* **1993**, 311.

(55) Goto, H.; Obata, S.; Nakayama, N.; Ohta, K. *CONFLEX 7*, CONFLEX Corporation: Tokyo, Japan, 2012.

(56) Goto, H.; Osawa, E. *J. Am. Chem. Soc.* **1989**, *111*, 8950.

(57) Frisch, M. J., Trucks, G. W., Schlegel, H. B., Scuseria, G. E., Robb, M. A., Cheeseman, J. R., Scalmani, G., Barone, V., Mennucci, B., Petersson, G. A., Nakatsuji, H., Caricato, M., Li, X., Hratchian, H. P., Izmaylov, A. F., Bloino, J., Zheng, G., Sonnenberg, J. L., Hada, M., Ehara, M., Toyota, K., Fukuda, R., Hasegawa, J., Ishida, M., Nakajima, T., Honda, Y., Kitao, O., Nakai, H., Vreven, T., Montgomery, J. A., Jr., Peralta, J. E., Ogliaro, F., Bearpark, M., Heyd, J. J., Brothers, E., Kudin, K. N., Staroverov, V. N., Keith, T., Kobayashi, R., Normand, J., Raghavachari, K., Rendell, A., Burant, J. C., Iyengar, S. S., Tomasi, J., Cossi, M., Rega, N., Millam, J. M., Klene, M., Knox, J. E., Cross, J. B., Bakken, V., Adamo, C., Jaramillo, J., Gomperts, R., Stratmann, R. E., Yazyev, O., Austin, A. J., Cammi, R., Pomelli, C., Ochterski, J. W., Martin, R. L., Morokuma, K., Zakrzewski, V. G., Voth, G. A., Salvador, P., Dannenberg, J. J., Dapprich, S., Daniels, A. D., Farkas, O., Foresman, J. B., Ortiz, J. V., Cioslowski, J., Fox, D. J. *Gaussian 09*, Revision B.01; Gaussian, Inc.: Wallingford, CT, 2010.

(58) McLean, A. D.; Chandler, G. S. *J. Chem. Phys.* **1980**, *72*, 5639.

(59) Saha, T.; Dasari, S.; Tewari, D.; Prathap, A.; Sureshan, K. M.; Bera, A. K.; Mukherjee, A.; Talukdar, P. *J. Am. Chem. Soc.* **2014**, *136*, 14128.

(60) Talukdar, P.; Bollot, G.; Mareda, J.; Sakai, N.; Matile, S. *J. Am. Chem. Soc.* **2005**, *127*, 6528.

(61) Gorteau, V.; Bollot, G.; Mareda, J.; Perez-Velasco, A.; Matile, S. *J. Am. Chem. Soc.* **2006**, *128*, 14788.

(62) Madhavan, N.; Robert, E. C.; Gin, M. S. *Angew. Chem., Int. Ed.* **2005**, *44*, 7584.

(63) Bochenska, M.; Biernat, J. F.; Topolski, M.; Bradshaw, J. S.; Bruening, R. L.; Izatt, R. M.; Dalley, N. K. *J. Inclusion Phenom. Mol. Recognit. Chem.* **1989**, *7*, 599.

(64) Biwersi, J.; Tulk, B.; Verkman, A. S. *Anal. Biochem.* **1994**, *219*, 139.

(65) Milano, D.; Benedetti, B.; Boccalon, M.; Brugnara, A.; Iengo, E.; Tecilla, P. *Chem. Commun.* **2014**, *50*, 9157.

(66) Tsukimoto, M.; Harada, H.; Ikari, A.; Takagi, K. *J. Biol. Chem.* **2005**, *280*, 2653.

(67) Yu, L.; Jiang, X. H.; Zhou, Z.; Tsang, L. L.; Yu, M. K.; Chung, Y. W.; Zhang, X. H.; Wang, A. M.; Tang, H.; Chan, H. C. *PLoS One* **2011**, *6*, e17322.

(68) Verkman, A. S. *Am. J. Physiol. Cell Physiol.* **1990**, *259*, C375.

(69) Zhu, Y.; Parsons, S. P.; Huizinga, J. D. *Neurogastroenterol. Motil.* **2010**, *22*, 704.

(70) Van Rossom, W.; Asby, D. J.; Tavassoli, A.; Gale, P. A. *Org. Biomol. Chem.* **2016**, *14*, 2645.

(71) Gottlieb, E.; Armour, S. M.; Harris, M. H.; Thompson, C. B. *Cell Death Differ.* **2003**, *10*, 709.

(72) Ly, J. D.; Grubb, D. R.; Lawen, A. *Apoptosis* **2003**, *8*, 115.

(73) Chu, Z.-L.; Pio, F.; Xie, Z.; Welsh, K.; Krajewska, M.; Krajewski, S.; Godzik, A.; Reed, J. C. *J. Biol. Chem.* **2001**, *276*, 9239.

(74) Druškovič, M.; Šuput, D.; Milisav, I. *Croat. Med. J.* **2006**, *47*, 832.

(75) Ashkenazi, A. *Nat. Rev. Drug Discovery* **2008**, *7*, 1001.

(76) Loreto, C.; La Rocca, G.; Anzalone, R.; Caltabiano, R.; Vespasiani, G.; Castorina, S.; Ralph, D. J.; Cellek, S.; Musumeci, G.; Giunta, S.; Djinovic, R.; Basic, D.; Sansalone, S. *BioMed Res. Int.* **2014**, *2014*, 1.

(77) Smiley, S. T.; Reers, M.; Mottola-Hartshorn, C.; Lin, M.; Chen, A.; Smith, T. W.; Steele, G. D.; Chen, L. B. *Proc. Natl. Acad. Sci. U. S. A.* **1991**, *88*, 3671.

(78) Cossarizza, A.; Baccaranicontri, M.; Kalashnikova, G.; Franceschi, C. *Biochem. Biophys. Res. Commun.* **1993**, *197*, 40.

(79) Liu, X.; Kim, C. N.; Yang, J.; Jemmerson, R.; Wang, X. *Cell* **1996**, *86*, 147.

(80) Li, P.; Nijhawan, D.; Budihardjo, I.; Srinivasula, S. M.; Ahmad, M.; Alnemri, E. S.; Wang, X. *Cell* **1997**, *91*, 479.

(81) Jiang, X.; Wang, X. *Annu. Rev. Biochem.* **2004**, *73*, 87.

(82) Cullen, S. P.; Martin, S. J. *Cell Death Differ.* **2009**, *16*, 935.

(83) Wu, J.; Liu, T.; Xie, J.; Xin, F.; Guo, L. *Cell. Mol. Life Sci.* **2006**, *63*, 949.

(84) McIlwain, D. R.; Berger, T.; Mak, T. W. *Cold Spring Harbor Perspect. Biol.* **2013**, *5*, a008656.

(85) de Vries, E. G. E.; Gietema, J. A.; de Jong, S. *Clin. Cancer Res.* **2006**, *12*, 2390.

(86) Haupt, S.; Berger, M.; Goldberg, Z.; Haupt, Y. *J. Cell Sci.* **2003**, *116*, 4077.

(87) Milczarek, G. J.; Martinez, J.; Bowden, G. T. *Life Sci.* **1996**, *60*, 1.

(88) Ekert, P. G.; Silke, J.; Vaux, D. L. *Cell Death Differ.* **1999**, *6*, 1081.

(89) Shah, N.; Asch, R. J.; Lysholm, A. S.; LeBien, T. W. *Blood* **2004**, *104*, 2873.

(90) Boulares, A. H.; Yakovlev, A. G.; Ivanova, V.; Stoica, B. A.; Wang, G.; Iyer, S.; Smulson, M. *J. Biol. Chem.* **1999**, *274*, 22932.

(91) Park, S.-H.; Choi, Y. P.; Park, J.; Share, A.; Francesconi, O.; Nativi, C.; Namkung, W.; Sessler, J. L.; Roelens, S.; Shin, I. *Chem. Sci.* **2015**, *6*, 7284.

(92) Curtin, N. J. *Nat. Rev. Cancer* **2012**, *12*, 801.

(93) O'Rourke, B.; Cortassa, S.; Aon, M. A. *Physiology* **2005**, *20*, 303.

(94) Zhao, W.; Lu, M.; Zhang, Q. *Mol. Med. Rep.* **2015**, *12*, 8041.

(95) Khodade, V. S.; Kulkarni, A.; Gupta, A. S.; Sengupta, K.; Chakrapani, H. *Org. Lett.* **2016**, *18*, 1274.

(96) Kim, E.-J.; Bhuniya, S.; Lee, H.; Kim, H. M.; Cheong, C.; Maiti, S.; Hong, K. S.; Kim, J. S. *J. Am. Chem. Soc.* **2014**, *136*, 13888.

(97) Simon, H. U.; Haj-Yehia, A.; Levi-Schaffer, F. *Apoptosis* **2000**, *5*, 415.

(98) Tsujimoto, Y.; Shimizu, S. *Apoptosis* **2007**, *12*, 835.

(99) Circu, M. L.; Aw, T. Y. *Free Radical Biol. Med.* **2010**, *48*, 749.

(100) Herrera, B.; Álvarez, A. M.; Sánchez, A.; Fernández, M.; Roncero, C.; Benito, M.; Fabregat, I. *FASEB J.* **2001**, *15*, 741.